Energy, Mines and Resources Canada

Énergie, Mines et Ressources Canada

CANMET

Canada Centre for Mineral and Energy Technology

Centre canadien de la technologie des minéraux et de l'énergie

Mining Research Laboratories

Laboratoires de recherche minière

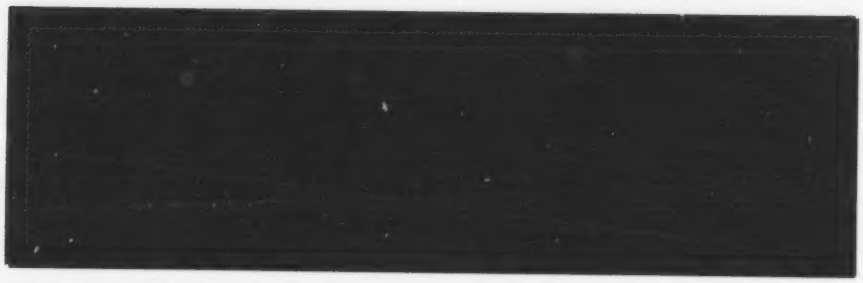

Canada

WAVEFORM ANALYSIS AND VELOCITY STRUCTURE AT QUIRKE MINE AND ADJACENT AREAS. PART 2: EXTENSION OF THE FAILURE ZONE

Shengzao Chen

MRL 90-130 (TR) *AUGUST 1990*

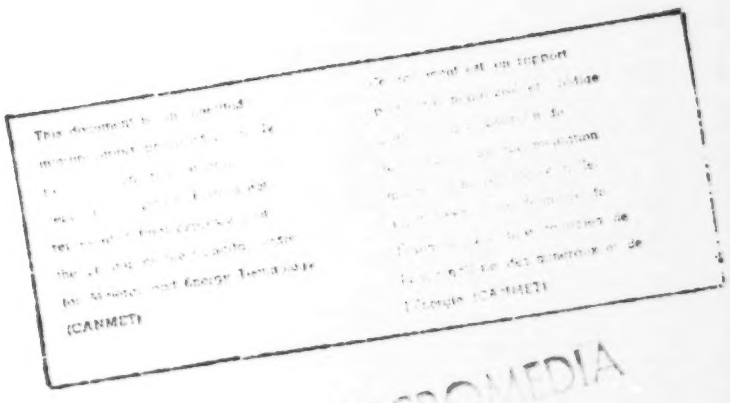

25 pp

MICROMEDIA

91-01605/

WAVEFORM ANALYSIS AND VELOCITY STRUCTURE AT QUIRKE MINE AND ADJACENT AREAS PART 2: EXTENSION OF THE FAILURE ZONE

Shengzao Chen

ABSTRACT

Of all the recorded 91 rockbursts from 1987 to 1989, 76 events were relocated or newly located in Quirke Mine and adjacent areas, and 93% of them occurred in Quirke Mine. The corner frequency shifts and slopes in the frequency domain show that the failure zone of Quirke Mine has higher values than Denison Mine, whereas the V_p/V_s ratios, Poisson's ratios and elastic moduli are lower. The central area of the failure zone around Site 1 exhibited a greater slowness (transit time), particularly in the S-wave, with a greater slowness difference to the exterior zone. These fractured features distinguish Quirke Mine from Denison Mine by the boundary pillar, i.e., the failure zone of Quirke Mine does not spread to Denison Mine.

Key words: Rockbursts; Waveform analysis; Seismic velocity; Failure zone.

*Post Doctoral Fellow, Elliot Lake Laboratory, CANMET, Energy, Mines and Resources Canada, Elliot Lake, Ontario, visiting from State Seismological Bureau, China.

ANALYSE DES FORMES D'ONDE ET STRUCTURE DES VITESSES A LA MINE QUIRKE ET DANS LES ENVIRONS PARTIE 2: AGRANDISSEMENT DE LA ZONE DE RUPTURE

Shengzao Chen*

RÉSUMÉ

Des 91 coups de toit enregistrés entre 1987 et 1989, 76 ont été relocalisés ou récemment situés à la mine Quirke et dans les environs, et 93% d'entre eux se sont produits à la mine Quirke. Les déplacements de fréquence de coin et les pentes dans le domaine fréquenciel indiquent que la zone de rupture de la mine Quirke présente des valeurs plus élevées qu'à la mine Denison, tandis que les rapports V_p/V_s, les coefficients de Poisson et les modules d'élasticité sont plus faibles. Le centre de la zone de rupture autour du Site 1 présentait une plus grande lenteur (temps de transit), notamment dans l'onde S, avec un plus grand écart de lenteur vers la zone extérieure. Ces éléments fracturés séparent la mine Quirke de la mine Denison par le pilier périmétrique; ainsi la zone de rupture de la mine Quirke ne s'étend pas jusqu'à la mine Denison.

---

* Boursier post-doctoral du Bureau sismologique d'État, Chine, invité au Laboratoire d'Elliot Lake, CANMET, Énergie, Mines et Ressources Canada. Elliot Lake, Ontario.

Mots clés: coup de toit, analyse des formes d'onde, vitesse sismique, zone de rupture

CONTENTS

	Page
ABSTRACT	i
RESUME	ii
INTRODUCTION	1
NEW LOCATIONS OF EVENTS	1
CORNER FREQUENCY SHIFTS AND SLOPES	2
SEISMIC VELOCITIES AND ELASTIC PROPERTIES	3
SLOWNESS DIFFERENCE	6
DISCUSSION	8
CONCLUSIONS	10
ACKNOWLEDGEMENTS	10
REFERENCES	10

TABLES

No.		
1.	The mean elastic constants at Quirke Mine	5
2.	A general relationship for V_p/V_s versus Poisson's Ratio (σ)	5

FIGURES

1.	The locations of 91 rockburst events at Quirke Mine and adjacent areas from 1987 to 1989	13
2.	The locations of 37 events in 1987 at Quirke Mine and adjacent areas	14
3.	Map showing the contours of the sum of residual travel times at Quirke Mine and adjacent areas	15
4.	Distribution of the corner frequency shifts (f_o^p/f_o^s) in Quirke Mine and adjacent areas	16
5.	Distribution of the slopes in plateau-frequency spectra at Quirke Mine and adjacent areas	17
6.	Distribution of V_p/V_s ratios at Quirke Mine and adjacent areas	18
7.	Distribution of the slowness differences between P- and S-waves at Quirke Mine and adjacent areas	19
8.	V_p versus V_s plot indicating lines of constant V_pV_s product and constant V_p/V_s ratio at Quirke Mine and adjacent areas	20
9.	Estimated error versus average velocity in the area studied	21

INTRODUCTION

Between August 1984 to the end of 1985 the pillar failure zone has spread from the centre to the exterior (1). Waveform analyses in frequency domain revealed the basic features of the failure zone (2). This paper deals with the extension of the failure zone in Quirke Mine, starting with a study of rockburst activity, velocity structure and the spatial distribution of the source parameters concerned with the characteristics of the failure zone.

NEW LOCATIONS OF EVENTS

From the calculation of P- and S-wave velocities for 37 events in 1987 at Quirke Mine, some incorrect locations were indicated, which resulted in too high velocities for both P- and S-waves at the failure zone. It is necessary when determining the extent of the fractured zone to relocate the hypocenters of the rockbursts at the mine, which will affect the spatial distribution of source parameters and the velocities determined from the events, and will influence judgement of the extent of the fractured zone.

Figure 1 shows the new locations of 91 events which occurred at Quirke Mine and adjacent areas during the period 1987 to 1989. The contours in the Figure indicate hypocentre elevations (in feet). Most of the events were determined using an optimization method with the sum of the residual travel times (SRT), and some, using the Block Program in this Laboratory. Twenty-two of thirty-seven events in 1987 were relocated, thirty-six in 1988, and eighteen in 1989 are newly located.

Ninety-three percent of the 91 events occurred at Quirke Mine, i.e., mining induced seismic activity of the Quirke Mine failure zone. In view of the timing of these events, it is evident that they have a tendency to concentrate in the Quirke Mine failure zone since 1987. The area of highly concentrated rockbursts is consistent with the range of the failure zone as determined by Hedley (1).

This paper studies the events in 1987, of which thirty-seven are indicated in Figure 2.

The contours of the sum of residual travel times from source to sensor sites are shown in Figure 3, from which the best fitted locations of events were chosen. To obtain the contours many 1 x 1 grids were made over the mine plane map, covering Quirke and Denison Mines. THe grid unit is taken as 100 feet within the area between 5 sensor sites, and 500 feet outside the area, respectively. For each event the sum of residual travel times is expressed by:

$$s = \Sigma \Delta t_i \qquad \text{Eq 1}$$

where, $\Delta t_i = t_i - t_o$ which represents the residual time at site i,

t_o indicates the minimum arrival time at the site, a reference station.

CORNER FREQUENCY SHIFTS AND SLOPES

The spatial distribution of f_o^p/f_o^s in Quirke Mine (Figure 4), shows that the failure zone is covered by high ratios, greater than 1.5, and particularly enclosed by a series of contours of approximately 1.7 to 2.0. Beyond the failure zone, the ratios are obviously limited to 1.5, usually they are from 1.1 to 1.5. The ratios through the boundary pillar are about 1.4 to 1.6 in Denison Mine, lower than in the Quirke Mine fractured zone.

The normal ratio of f_o^p/f_o^s is 1.46 for $\alpha/\beta = \sqrt{3}$ (2). Much higher ratios in Quirke Mine imply fractured features, and the higher ratio contours drop off in the failure zone.

The f_o^p/f_o^s ratios are more dispersed in the failure zone than in the outside zone and do not display an exactly consistent tendency of higher f_o^p/f_o^s versus the higher α/β. Except for the calculated deviations from the seismic source models, the most probable interpretation of the dispersion of f_o^p/f_o^s is that the corner frequency shifts are not only related to the source properties, but are also related to the medium properties that affect the

seismic wave propagation.

Figure 5 shows high slopes of over 3.5 in absolute values of the failure zone at Quirke Mine which is separated from Denison Mine by the boundary pillar. The high slopes are contrasted with the high corner frequency shifts at the failure zone, and the area covered by these high values is approximately consistent.

SEISMIC VELOCITIES AND ELASTIC PROPERTIES

The seismic velocity at site i, V_i, is calculated as follows:

$$V_i = R_i/t_i \qquad \text{Eq 2}$$

where, R_i = distance from source to site i,

$t_i = t_o + \Delta t_i$, in which $t_o = R_o/V_o$ represents the relative travel time at which the seismic wave travels the shortest distance, R_o, from source to the reference station at an average velocity of V_o, and Δt_i is the travel time difference between site i and the reference station.

For all the calculated 32 events of 37 in Quirke Mine, of which events 3, 5, 6, 7 and 18 are omitted because of too small a residual time which leads to too high velocities, the average velocities are obtained by:

$$V_j = \Sigma_i^N V_{ji}/N \qquad \text{Eq 3}$$

Considering V_o^s = 3660 m/s for S-waves, the calculated velocities range from 3350 to 3450 m/s around site 1 at the failure zone, to some extent lower than the average. Using the average velocity V_o^p = 5940 and 5600 m/s for the P-wave, the calculated velocities are higher than the average, which is in contradiction to the fractured feature that should appear in the failure zone. For most events, the minimum residual travel time sums were reached at first iteration. Since the velocities for P- and S-waves are dependent to some degree on the choice of initial average velocity, it is reasonable to use the V_p/V_s ratio which is an independent characteristic of the velocity structure.

Figure 6 shows the distribution of V_p/V_s ratios in a range from 1.42 to 1.74. The low ratios of less than 1.68 are obviously concentrated in the failure zone, which is new evidence for the fractured media in Quirke Mine. The area covered by the low V_p/V_s ratios is much more consistent with the extension of the failure zone in the mine. Around site 1, the V_p/V_s ratio is relatively higher than the average value of 1.62 (2) mainly because of the lower S-wave velocity there.

When converting propagation velocities of elastic waves to elastic constants concerning the medium properties, and vice versa, the fundamental equations of the elasticity theory and the definition of the Lame coefficients (μ, and λ) are as follows:

$$\mu = \rho V_s^2 = G \qquad \text{Eq 4}$$

$$\lambda = \rho V_p^2 - 2\rho V_s^2 \qquad \text{Eq 5}$$

$$E = \frac{\mu(3\lambda + 2\mu)}{\lambda + \mu} \qquad \text{Eq 6}$$

$$\sigma = \frac{\lambda}{2(\lambda + \mu)} = \frac{\gamma^2 - 2}{2(\gamma^2 - 1)} \qquad \text{Eq 7}$$

$$K = \lambda + \frac{2}{3}\mu \qquad \text{Eq 8}$$

$$V_p = \sqrt{\frac{\lambda + 2\mu}{\rho}} = \sqrt{\frac{K + 4\mu/3}{\rho}} \qquad \text{Eq 9}$$

$$V_s = \sqrt{\frac{\mu}{\rho}} \qquad \text{Eq 10}$$

$$Vp_M = \sqrt{\frac{E(1 - \sigma)}{\rho(1 + \sigma)(1 - 2\sigma)}} \qquad \text{Eq 11}$$

where, μ and λ are the Lame coefficients

V_p and V_s are the propagation velocities of the longitudinal and transverse elastic waves, i.e., P- and S-waves

$\gamma = V_p/V_s$

E is Young's modulus

G is the shear modulus

K is the bulk modulus

σ is Poisson's ratio

ρ is the density, and

Vp_M is P-wave velocity in an infinite medium.

From the average elastic velocities V_p = 5600 m/s, and V_s = 3660 m/s, the mean elastic constants are evaluated in Table 1. The relationships between V_p/V_s and Poisson's ratio (σ) are calculated in a broad value range, as shown in Table 2.

For the normal medium in most circumstances we have $V_p/V_s = \sqrt{3}$, and so σ = 0.25. However, when using the elastic constants in Table 1 for Quirke Mine, the average Poisson's ratio is as low as σ = 0.13, corresponding to V_p/V_s = 1.53. For V_p/V_s = 1.45 to 1.68 in the failure zone, the Poisson's ratio (σ) ranges from 0.05 to 0.23. In general, we find $\sigma \leq 0.25$, and for most parts of Quirke Mine $\sigma < 0.25$. This distinctly manifests the fractured features of the mine.

Table 1 - The mean elastic constants at Quirke Mine

$G(\mu)$	λ	E	K	Vp_M
3.62	1.23	8.16	3.64	6.02

*Data units in 10^{11} dyne/cm^2 for $G(\mu)$, λ, E, K; km/s for Vp_M.

Table 2 - A general relationship for V_p/V_s versus Poisson's Ratio (σ).

V_p/V_s	1.45	1.50	1.55	1.60	1.65	1.70	$\sqrt{3}$	1.75	1.80	1.85	1.90	1.95	2.00
σ	0.05	0.10	0.14	0.18	0.21	0.24	0.25	0.26	0.28	0.29	0.31	0.32	0.33

The elastic properties of rocks at Quirke Mine (Tables 1 and 2) are comparable with other results. For most quartzitic sandstones and quartzites in the USSR the modulus E ranges from 6.5 x 10^{11} to 8.69 x 10^{11} dyne/cm^2; the shear modulus G from 3.68 x 10^{11} to 3.82 x 10^{11} dyne/cm^2; and the Poisson's

ratio σ from 0.04 to 0.18 (3,4). In the Elliot Lake area, the modulus deformation, E, for conglomerate and quartzite individually range from 8.6 x 10^6 to 13.2 x 10^6 psi, and 9.2 x 10^6 to 11.2 x 10^6 psi (5), which are in agreement with 5.93 x 10^{11} to 9.10 x 10^{11} dyne/cm^2 and 6.34 x 10^{11} to 7.72 x 10^{11} dyne/cm^2, respectively.

From the standpoint of sedimentary formations, all U-deposits of commercial importance in the Blind River/Elliot Lake area are in the Matinenda formation which originated in the Elliot Lake Precambrian era (6). The conglomerate, quartz-pebble conglomerate and limestone contained in these formations throughout the Elliot Lake group, Hough Lake group upwards to the Quirke Lake group, show traces of uranium. The elastic constants derived from the seismic velocity at Quirke Mine are strongly supported by the test results for similar rock formations, as mentioned above.

In physics, the modulus E is a measure of the stiffness of rocks, or its ability to resist deformation within the proportional limit of the material. The greater the modulus of elasticity, the less deformation for any unit stress not exceeding the proportional limit. The modulus G is similar to that for tension or compression, but the deformation is in the direction of the shear plane of the rock body. For metals, the shear modulus of elasticity is approximately 0.4 times the tensile modulus of elasticity. Table 1 shows the ratio G/E = 0.44 as an average in Quirke Mine.

SLOWNESS DIFFERENCE

The slowness, or transit time (1/V), can be approximately derived from the travel time curve for homogeneous media in a very limited area. For laterally varying velocity structures, least-square iteration methods with travel time inversion and amplitude inversion have been developed by seismologists in recent years (7,8).

The slowness difference for P- and S-waves can be expressed by:

$$1/V_s - 1/V_p = \Delta t_{sp}/R \qquad \text{Eq 12}$$

where, $\Delta t_{sp} = t_s - t_p$, i.e., the travel time difference between P- and S-waves.

As P-waves propagate through the medium faster than S-waves, the further the distance, the greater the travel time difference. As shown in Figure 7, the lower slowness differences over most parts of the Quirke Mine failure zone, between 5 sensor sites, are consistent with the travel time records and the lower V_p/V_s ratio in the mine. Around Site 1, the greater slowness differences, from 1.12×10^{-4} to 1.2×10^{-4} s/m, are due to the large travel time difference that may result from the highly fractured medium, and/or the high porosity of the rocks which has a greater effect on the S-wave velocity than on that of the P-wave.

Transforming Equation 12 produces the following form:

$$1/V_s - 1/V_p = (V_p/V_s - 1)/V_p = (V_p - V_s)/(V_pV_s) \qquad \text{Eq 13}$$

which is obviously related to V_p/V_s ratio or V_pV_s product. The V_p/V_s ratio and V_pV_s product are superimposed on the plot of V_p against V_s at Quirke Mine and adjacent areas (Figure 8). These lines are proven to be perpendicular when $V_p = V_s$, and form an angle of 70^o when $V_p = 1.5\ V_s$. In general, the V_p/V_s lines have slope γ, a constant, while the V_pV_s lines have slope $-\gamma$ (9).

Various gross lithologies can be separated by lines of constant V_p/V_s ratio (10). Carbonates exhibit ratio values of about 1.9 to 1.8, and silica-rich sandstones about 1.7 or lower. The ratio, γ, typically ranges from 1.6 to 2.1 for sands, carbonates, and shales (9). Identification of lithology is very important for seismic exploration (11), but the development of porosity is even more critical.

Porosity is related to seismic velocity, although the precise relationship is dependent on rock type, clay content, fluids present, and different pressure/temperature. The relationships could be expressed by a variety of formulae depending on geological background, such as the one published by Castagna (12). Generally, high transit times indicate high

porosity (9). From Equation 13, for a specific type of rock or the same underground geological condition, the V_p/V_s ratio and V_pV_s product should be the same, so the slowness difference is dependent on the V_p or $V_p - V_s$, the velocity difference for P- and S-waves. It is worthwhile emphasizing that some regions of the world (e.g., the Gulf of Mexico coast) contain shales with very high transit times. Such shales would be difficult to distinguish from high-porosity carbonates on only a V_pV_s basis (9).

In Quirke Mine the configuration of the contour lines of slowness difference displays the failure zone as different to the outskirts of the area, of which the high transit times for S-waves around Site 1 make the slowness difference distinguishably higher than the outside zone.

A new diamond drill hole, directly over the centre of the seismicity affected area, encountered open vertical fractures between the mine workings and the beds 355 m above, of which the open gaps occurred at depths of 155 m, 234 m, and 255 m (13). These fractured rock bodies or beds will increase rock porosity which will undoubtedly result in anomalous observations of transit times.

DISCUSSION

We use α and β to represent P- and S-wave velocity in some special theoretical studies such as waveform analysis and elastic properties where the velocity is considered as a constant, but when studying the velocity structure it is customary to use V_p and V_s as physical quantities.

It will be seen that $f_o^p/f_o^s \leq \alpha/\beta$ from the assumption of $r_o^p/r_o^s = 1$. However, anomalous observations of $f_o^p/f_o^s > \alpha/\beta$ were found in the Quirke Mine failure zone.

The general relationship between f_o^p/f_o^s and α/β should be expressed by

$$f_o^p/f_o^s = (k_p/k_s)(\alpha/\beta)(r_o^s/r_o^p) \qquad \text{Eq 14}$$

where, k_p and k_s are constant coefficients for P- and S-waves. When $k_p = k_s$

and $r_o^s = r_o^p$ we get $f_o^p/f_o^s = \alpha/\beta$, the limited case. We use the relationship $f_o^p/f_o^s = 0.84\ \alpha/\beta$ in Quirke Mine for $k_p = 1.97/2\pi$, rather than $2.34/2\pi$ which is commonly used for S-waves, and in some cases for P-waves (14). Assuming $\alpha/\beta = \sqrt{3}$ for an homogeneous and isotropic medium, the normal value of f_o^p/f_o^s should be 1.46 (2). The calculated V_p/V_s ratios are less than, $\sqrt{3}$ at the failure zone, which means that the corner frequency shift could be lower than the observations at the mine. The interpretation of such a high corner frequency shift appears to be elastic scattering of the fractured medium in the mine. Furthermore, the dependent relationship of corner frequency shift to velocity may not be a simple linear relationship, and needs further study.

The choice of initial velocity models is important for inversion of a real velocity structure at the mine. Choosing $V_s = 3660$ m/s, the minimum estimated errors of hypocenters (rockburst event locations) requires an average velocity in the range 5490 to 6090 m/s which are very scattered. Two best-fitted average velocity values of 5940 m/s were found for events 31 (Figures 2 and 9), and 35 (Figure 2), but for most events it was hard to find a unique best-fitted velocity as an initial value. When considering most events and their shallow-foci we use 5600 m/s as an initial velocity for P-wave calculation and use the V_p/V_s ratio as a result to avoid or reduce the influence of the initial velocity on the calculated results. Thus we believe that the V_p/V_s ratios are valid enough to discuss the velocity structure at the mine. When we know the V_p/V_s ratios we can evaluate the velocities of P- and S-waves from the V_pV_s product in Figure 8.

The analysis of elastic properties implies that the average velocities $V_p = 5600$ m/s and $V_s = 3660$ m/s seem feasible for the fractured zone at Quirke Mine, but the higher calculated velocities, particularly in the P-wave is still puzzling. One possible interpretation can be made, i.e., relative high velocity in the lower velocity background of the failure zone may still have a potential for rockbursting. This implies highly stressed rock masses at some

parts of the failure zone in the mine. Further study of the velocity structure at the mine should involve the tomography technology in seismological inversion, and needs great enhancing with more available measurements of underground stresses.

CONCLUSIONS

The failure zone of Quirke Mine shows high corner frequency shifts, high slopes, high slowness, and/or alternate lower slowness, and also displays the lower Poisson's ratios and elastic modulus. These features distinguish Quirke Mine from the adjacent Denison Mine by the boundary pillar, i.e., the failure zone of Quirke Mine does not spread to Denison Mine.

ACKNOWLEDGEMENTS

This paper was supervised and reviewed by Dr. D.G.F. Hedley. The author wishes to thank Messrs. P. Rochon, M. Plouffe, and T.P. Lim for familiarizing me with computer systems in the Laboratory. Special thanks are given to Dr. R. Tervo and P. Rochon for reviewing this manuscript. All office staff are thanked for their cooperation. The study was funded by NSERC.

REFERENCES

1. Hedley, D.G.F., Roxburgh, R.W., and Muppalaneni, S.N., "A case history of rockbursts at Elliot Lake"; Proc 2nd Int Conf Stability in Underground Mines, Lexington, Kentucky, 1984.

2. Chen, S.Z., and Hedley, D.G.F., "Waveform analysis and velocity structure at Quirke Mine and adjacent areas. Part 1 - Source parameters for evidence of the failure zone"; Division Report MRL 90-117(TR), CANMET, Energy, Mines and Resources Canada, 1990.

3. Belikov, B.P., Zalesskii, B.V., Rozanov, Y.A., Sanina, E.A., and Timchenko, I.P., "Methods of studying the physicomechanical properties of rocks"; In: Physical and Mechanical Properties of Rocks, Zalesskii, B.V.

(Ed.), pp 1-58, Jerusalem, Israel, 1967.

4. Zalesskii, B.V., Silaeva, O.I., Korotkova, O.N., Likhacheva, Y.S., Nikolaev, S.V., and Andreeve, V.N., "Dynamic elasticity characteristics of certain minerals and monomineralic aggregates"; In: Physical and Mechanical Properties of Rocks, Zalesskii, B.V. (Ed.), pp. 117-123, Jerusalem, Israel, 1967.

5. Coates, D.F., Bielenstein, H.U., and Hedley, D.G.F., "A rock mechanics case history of Elliot Lake"; Division Report IR 72/53, CANMET, Energy, Mines and Resources Canada, 1972.

6. Robertson, J.A., "The Blind River uranium deposits: the ores and their setting"; Miscellaneous Paper 65, Ontario Ministry of Natural Resources, 1976.

7. Spencer, C. and Gubbins, D., "Travel time inversion for simultaneous earthquake location and velocity structure determination in laterally varying media"; Geophys J R Astr Soc vol. 63, No. 1, pp. 95-116, 1980.

8. Thompson, C., "Ray-theoretical amplitude inversion for laterally varying velocity structure below NORSAR"; Geophys J R Astr Soc, vol. 74, No. 2, pp. 525-558, 1983.

9. Iverson, W.P., Fahmy, B.A., and Smithson, S.B., "V_pV_s from mode-converted P-SV reflections"; Geophysics, vol. 54, No. 7, pp. 843-852, 1989.

10. Tatham, R.H., "V_p/V_s and lithology"; Geophysics, vol. 47, pp. 336-344, 1982.

11. McCormack, M.D., Dunbar, J.A., and Sharp, W.W., "A case study of stratigraphic interpretation using shear and compressional seismic data"; Geophysics, vol. 49, pp. 509-520, 1984.

12. Castagna, J.P., Batzle, M.L., and Eastwood, R.L., "Relationships between compressional-wave and shear-wave velocities in clastic silicate rocks"; Geophysics, vol. 50, pp. 571-581, 1985.

13. Brehaut, C.H., Hedley, D.G.F., "1987-1988 Annual report of the Canada-Ontario-Industry rockburst project"; Special Report SP 88-22E, pp. 1-22, CANMET, Energy, Mines and Resources Canada, 1989.

14. Hanks, T.C., "The corner frequency shift, earthquake source models and Q"; Bull Seismol Soc Am, vol. 71, No. 3, pp. 597-612, 1981.

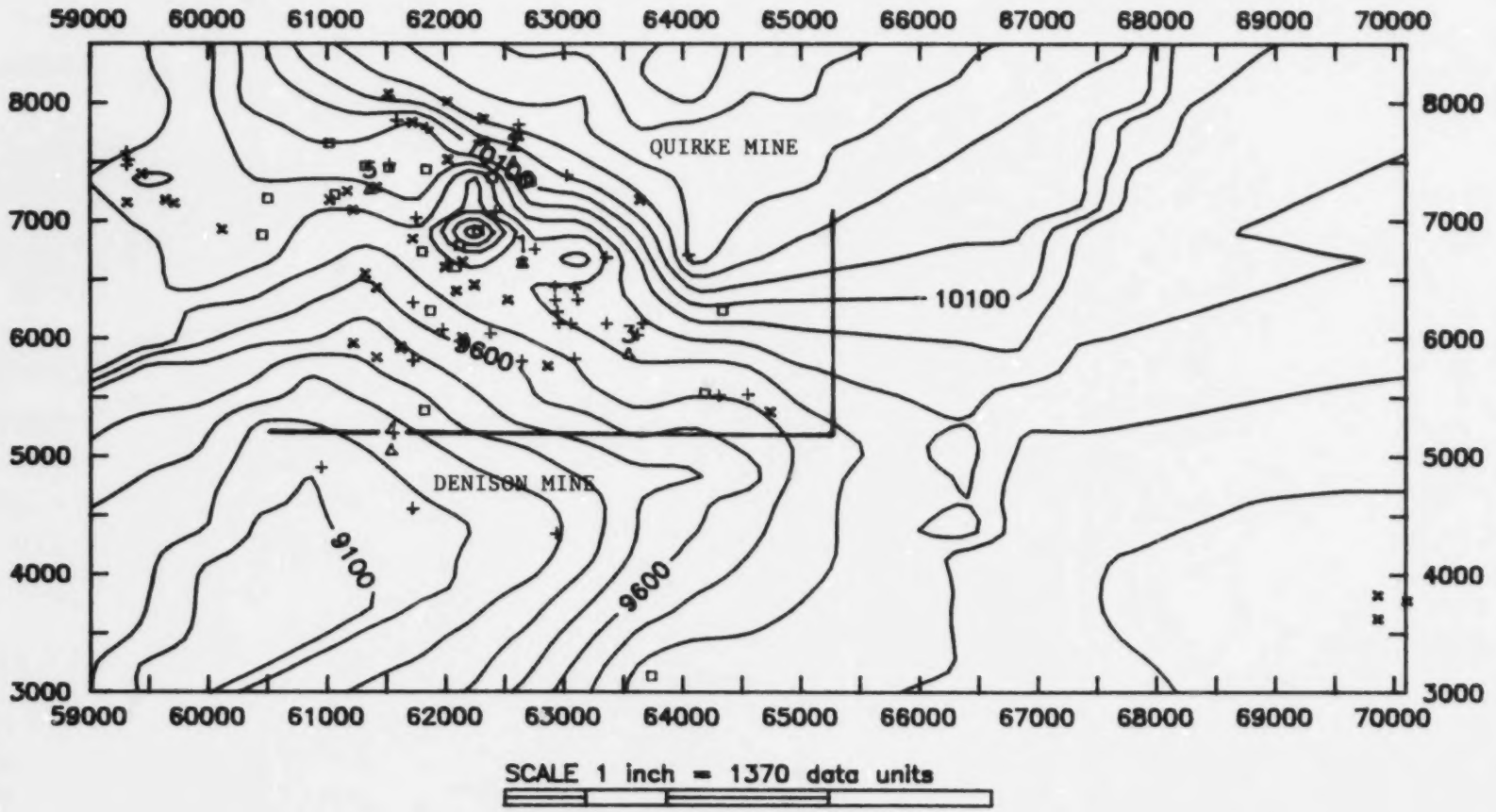

Fig. 1 - The locations of 91 rockburst events at Quirke Mine and adjacent areas from 1987 to 1989. (x) indicates 37 events in 1987; (+) indicates 36 events in 1988; and (□) indicates 18 events in 1989. Numbers 1 to 5 indicate sensor sites at the failure zone, site 4 is on the Denison Mine side.

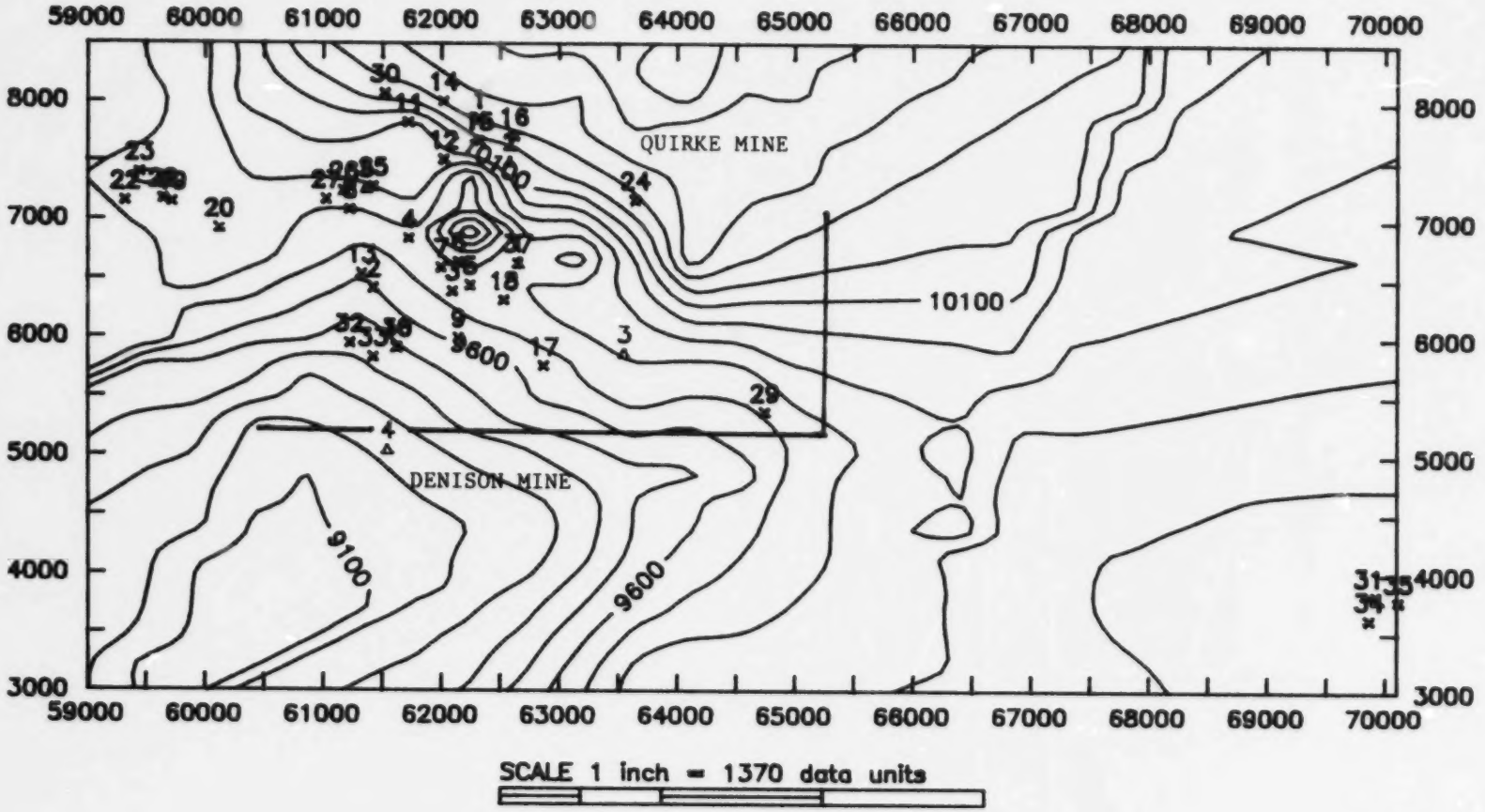

Fig. 2 - The locations of 37 events in 1987 at Quirke Mine and adjacent areas.

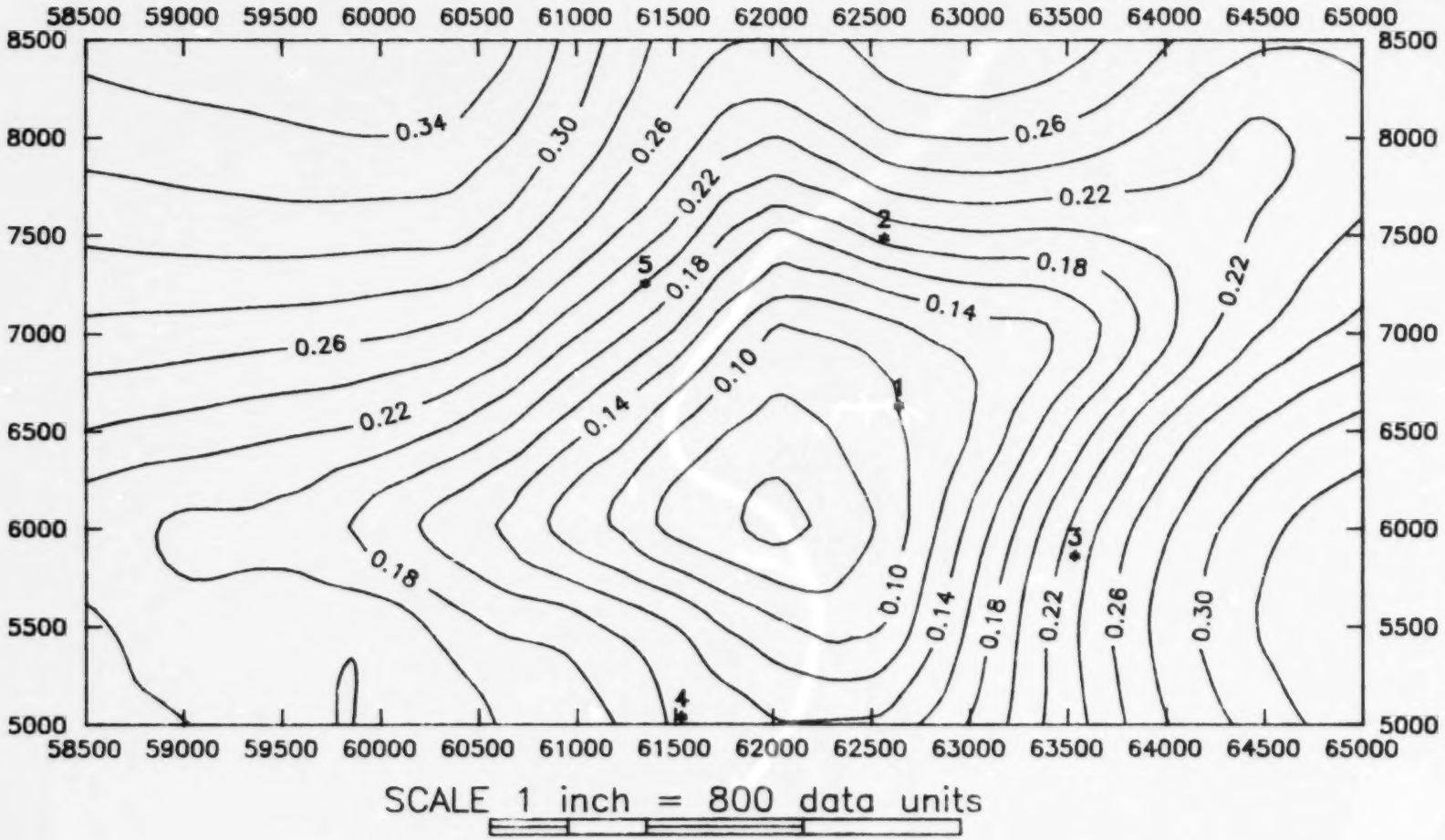

Fig. 3 - Map showing the contours of the sum of residual travel times at Quirke Mine and adjacent areas.

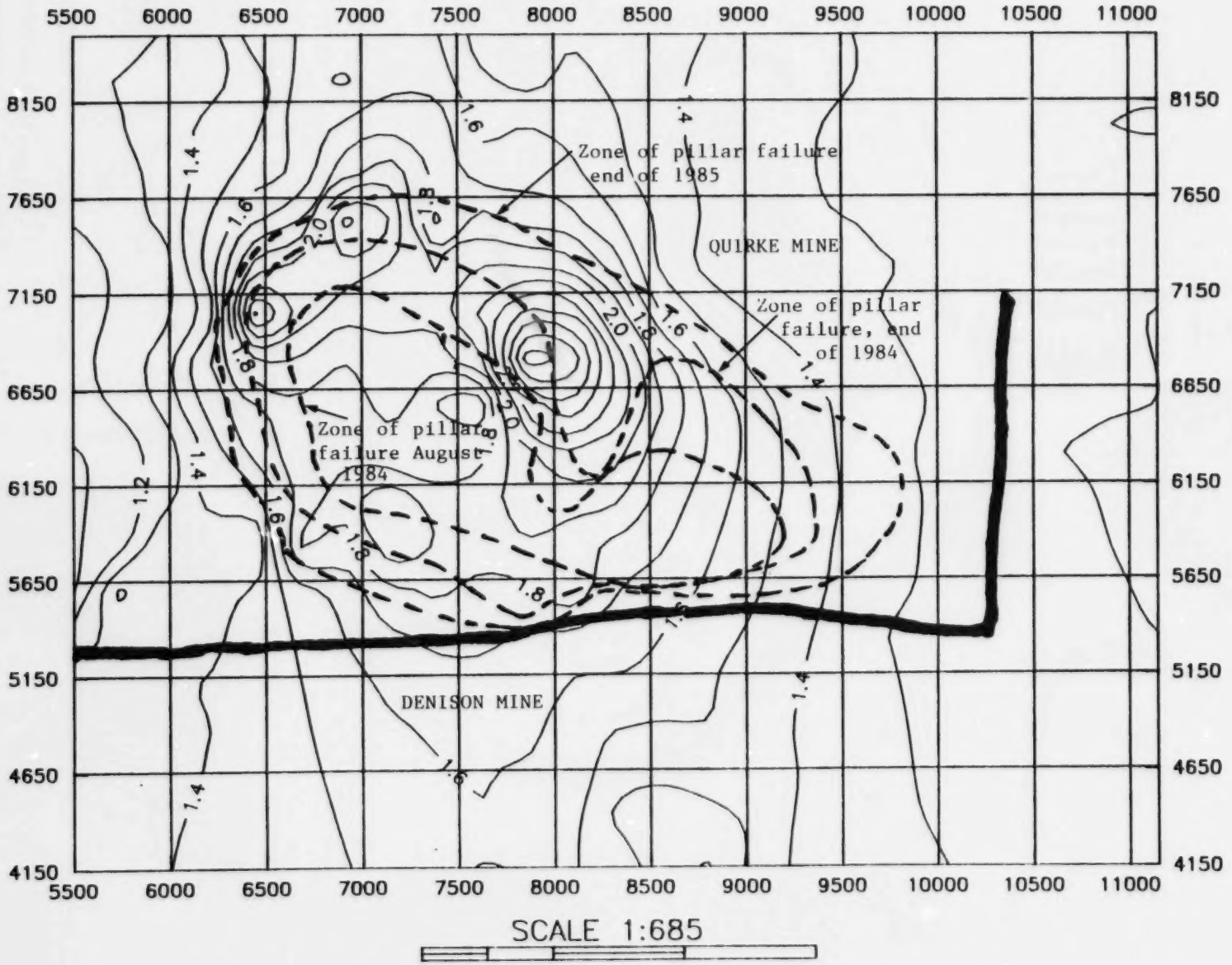

Fig. 4 - Distribution of the corner frequency shifts (f_o^p/f_o^s) in Quirke Mine and adjacent areas.

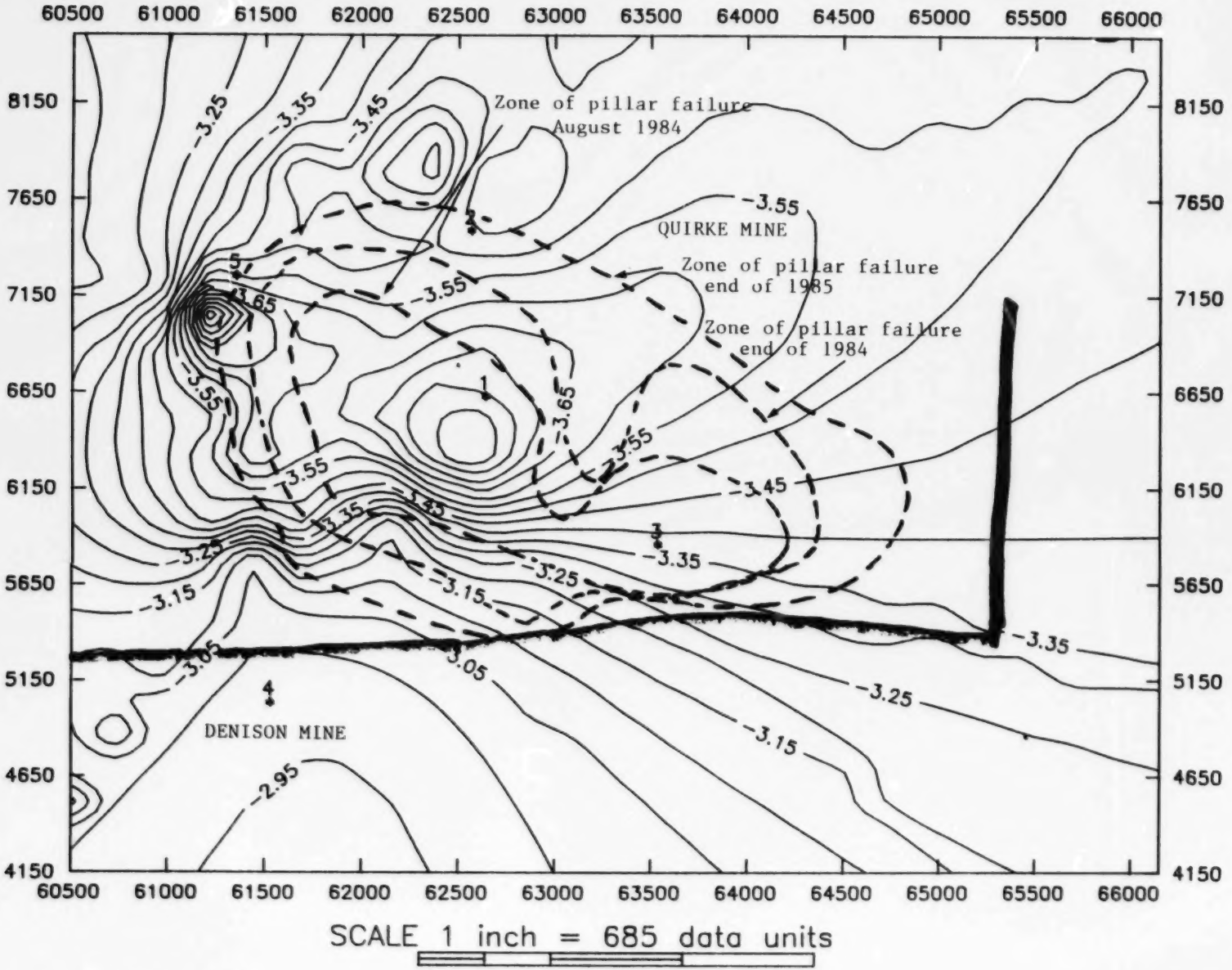

Fig. 5 - Distribution of the slopes in plateau-frequency spectra at Quirke Mine and adjacent areas.

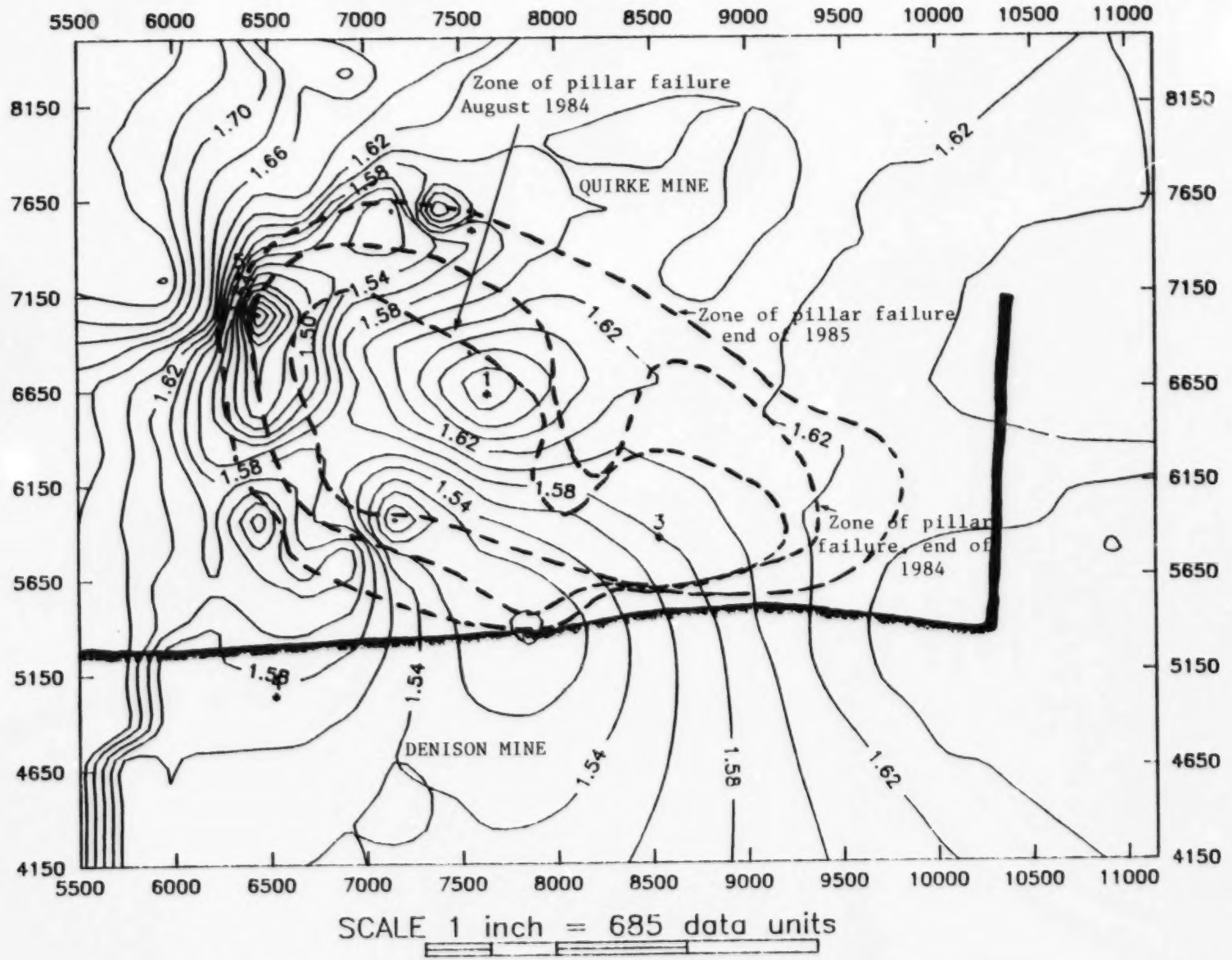

Fig. 6 - Distribution of V_p/V_s ratios at Quirke Mine and adjacent areas.

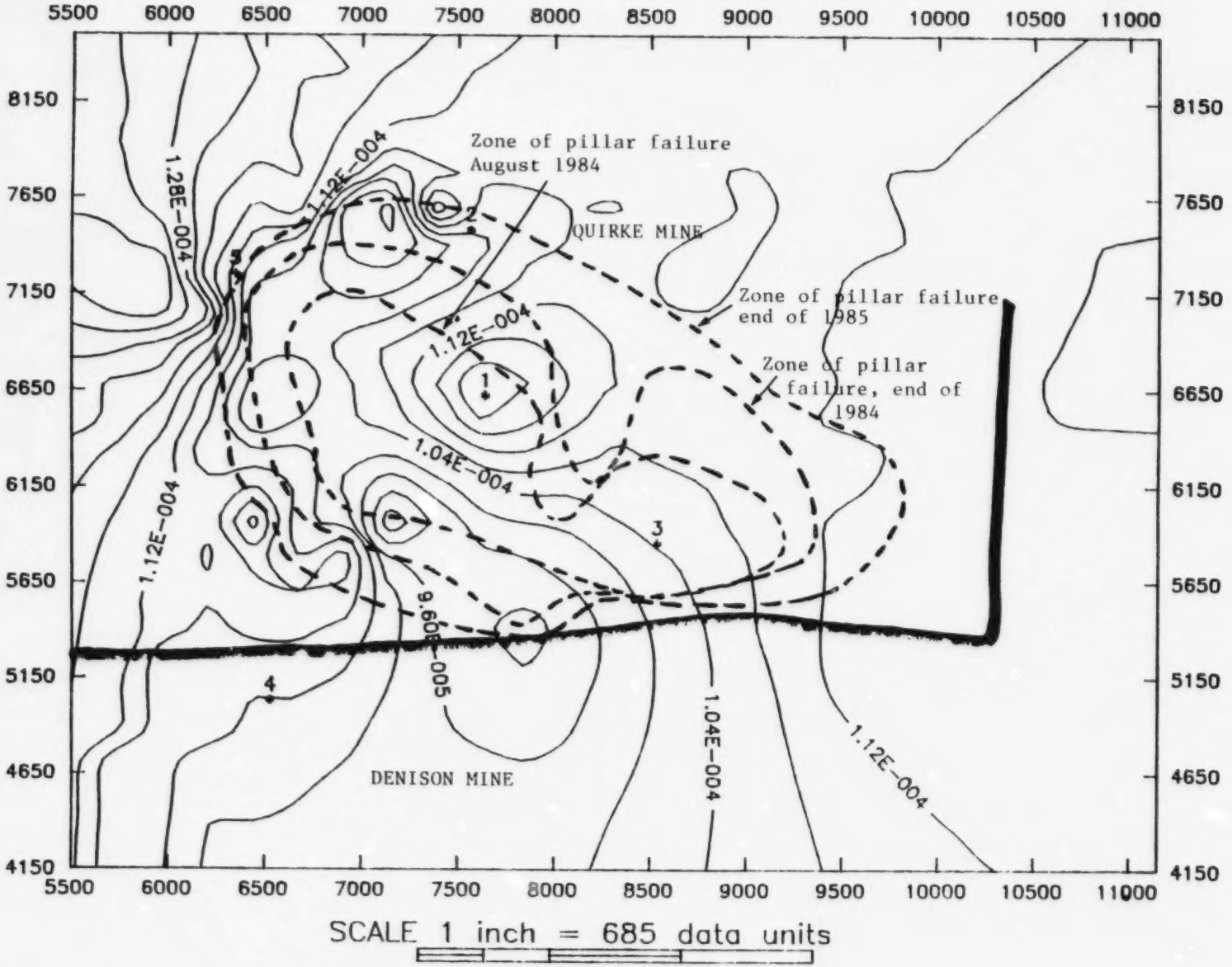

Fig. 7 - Distribution of the slowness differences between P- and S-waves at Quirke Mine and adjacent areas.

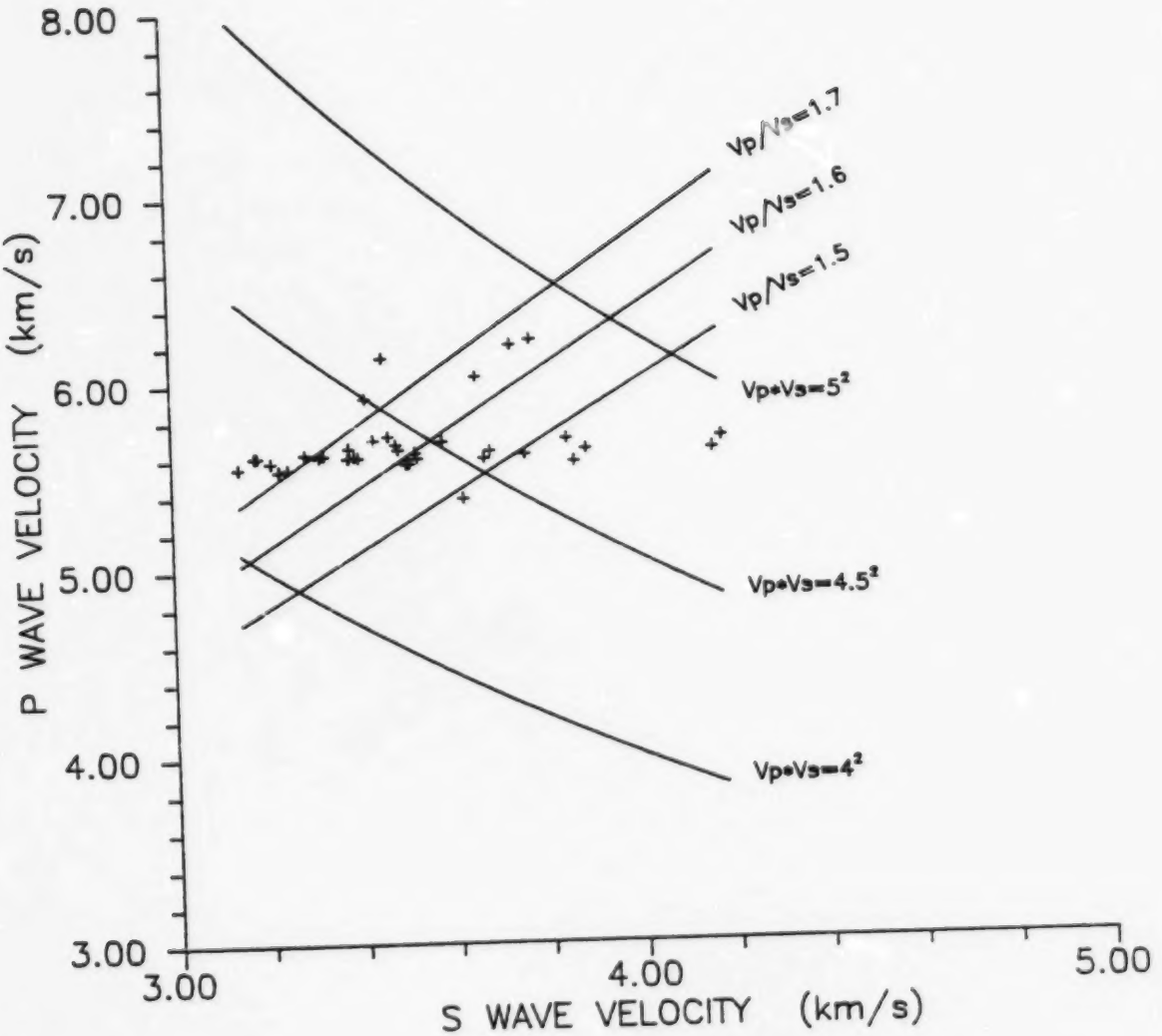

Fig. 8 - V_p versus V_s plot indicating lines of constant V_pV_s product and constant V_p/V_s ratio at Quirke Mine and adjacent areas.

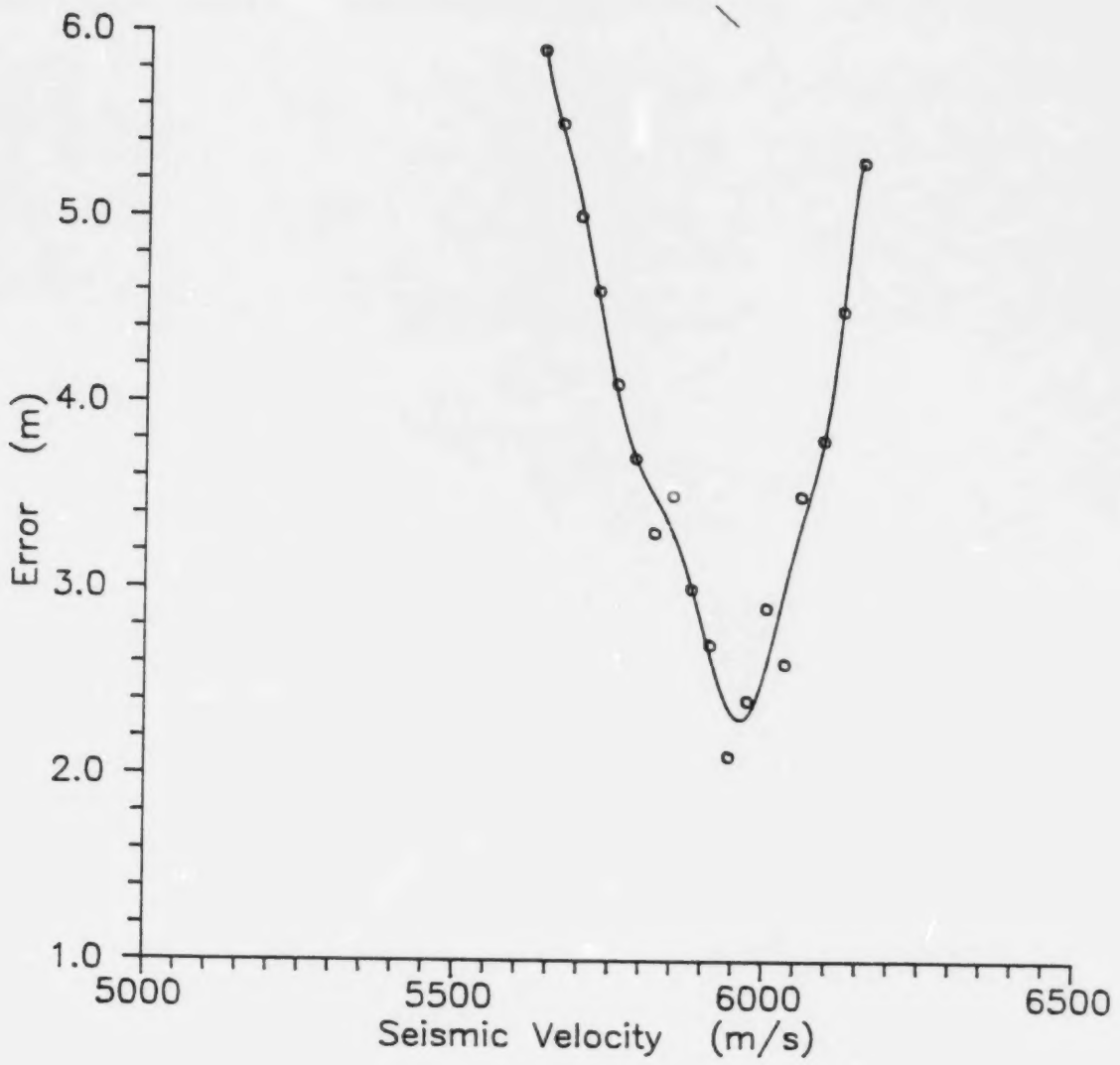

Fig. 9 - Estimated error versus average velocity in the area studied.